

Soil and Vegetation Patterns Along a Toposequence in a Dolomite Peak-cluster Depression Catchment

Qingmei Meng

Institute of Subtropical Agriculture Chinese Academy of Sciences

Zhiyong Fu (✉ zyfu@isa.ac.cn)

Institute of Subtropical Agriculture Chinese Academy of Sciences <https://orcid.org/0000-0002-8996-1179>

Sheng Wang

Institute of Subtropical Agriculture Chinese Academy of Sciences

Hongsong Chen

Institute of Subtropical Agriculture Chinese Academy of Sciences

Research Article

Keywords: dolomite, soil catena, nutrient stocks, vegetation patterns, soil-epikarst system

Posted Date: November 8th, 2021

DOI: <https://doi.org/10.21203/rs.3.rs-1036345/v1>

License: © ⓘ This work is licensed under a Creative Commons Attribution 4.0 International License.

[Read Full License](#)

16 **Abstract:**

17 *Aim* A deeper understanding of relationships between soil and vegetation is a
18 prerequisite for accelerating karst area vegetation restoration. Remarkable
19 achievements have been made at regional and individual plant scales, but research on
20 the relationship between soil and vegetation is insufficient at the hillslope catena scale
21 in karst areas.

22 *Methods* Soils and vegetation were investigated along a toposequence (upper-,
23 middle-, lower-slope, and depression) of a dolomite peak-cluster depression catchment.

24 *Results* A continuous soil catena pattern was developed along the toposequence.
25 From the top to bottom of soil catena, soil thickness, fine soil mass ratio, nutrient stocks,
26 and epikarst thickness gradually increased, while gravel mass ratio, pH, and saturated
27 hydraulic conductivity gradually decreased. However, nutrient contents showed no
28 significant change trends along the soil catena. There was a strong spatial association
29 between soil types and dominant vegetation communities. The associations were as
30 follows: herbs associated with entisols in the upper-slope; herbs and shrubs with
31 inceptisols in the middle-slope; shrubs with semi-alfisols in the lower-slope; and trees
32 with alfisols in the depression.

33 *Conclusions* The dolomite rocks displayed an evenly progressive karstification
34 process. This led to an undeveloped underground karstic network incapable of
35 transporting soil materials into underground. Soil materials still accumulated at
36 different topographic positions surface and formed a continuous catena. Parameters for
37 nutrient stock may be more suitable for assessing soil productivity and to guide
38 vegetation restoration key factors in karst regions than nutrient content parameters.

39 **Keywords:** dolomite; soil catena; nutrient stocks; vegetation patterns; soil-epikarst

40 system

41 **1. Introduction**

42 A toposequence is a spatial object that maintains flow connectivity from summit or
43 hillslope initiation to base, or hillslope conclusion. Catenary soils usually developed
44 along a toposequence because the degree of transport and deposition of particulate
45 constituents in the soil profile differs among soils with different topographic positions
46 (Schlichting 1970; Brunner et al. 2004; Lozano-García and Parras-Alcántara, 2014).

47 Generally, upper-slope erosion and accompanying lower-slope sedimentation result
48 in gradual soil layer and regolith thickening from the upper-slope to the depression.
49 Regular changes of regolith thickness and soil profile morphological characteristics
50 along a topographic gradient are represent as the primary conceptual model for the soil
51 catenary process (Sommer and Schlichting 1997; Applegarth and Dahms 2001;
52 Lozano-García and Parras-Alcántara 2014). The catena concept indicates soil-
53 vegetation combination spatial patterns located on a specific landform. However, soil
54 and vegetation characteristics can vary significantly along a toposequence among at
55 different environment factors such as parent materials, climate, topography and human
56 activities (Boling et al. 2008; Podwojewski et al. 2011).

57 Karst peak-cluster depression is a special geomorphic unit surrounded by slopes
58 which, within a very short horizontal distance, shows rapid changes, from, for example,
59 a close-to-90° -cliff to a relatively flat depression. Potential energy decreases sharply
60 from the slope top to the depression leading to a remarkable potential gradient between
61 the slope part and the depression part. Spatially, soils and vegetations in this unique
62 peak-cluster depression system have the topographic and hydrological conditions to

63 form a catenary pattern. However, for the karst landscape, knowledge about the soil-
64 vegetation relationships were mostly relied on the results carried out in regional or plant
65 individual scales. Related studies in catchment or catenary scales are relative rare due
66 to the ubiquitous extremely high structural heterogeneity in these scales. For instance,
67 in karst regional scale, Jiang et al. (2014) found that bedrock geochemistry via
68 influencing the regolith water-retention capacities determined the karstic vegetation
69 productivity. In individual plant scale, karstic site-specific characteristics such as
70 bedrock outcrops extent and soil thickness were the main controlling environment
71 factors and determining plant community composition (Liu et al. 2019). Thin soils were
72 dominated by shallow-rooted plants preferring surface soil water, while continuous
73 carbonate rock outcrops were usually dominated by deep-rooted plants preferring rock
74 crevices water (Nie et al. 2010, Ding et al. 2020). Considering that hillslopes and
75 catchments are often as basic management units for implementing ecological
76 restoration in severely degraded karst ecosystems (Jiang et al. 2014), there is a strong
77 need to conduct works to bridge the perception gap in the catenary scale.

78 Moreover, with regard to the soil forming characteristics of karst slope land, through
79 extensive implementation of pedon scale excavation at the complete landform scale of
80 peak-cluster depressions, systematic studies on soil formation processes and soil catena
81 patterns are also still insufficient. Scholars generally believe that the high Ca and Mg
82 content of carbonate rocks and unique karstification processes hinder the loss of salt-
83 based components in soil and desilicification and allitization. Researchers usually
84 regard calcareous soil as a soil category in entisols. There are four sub-categories of
85 calcareous soils: black; brown; yellow; and, red calcareous soil. Typically they are
86 shallow, not obviously stratified, clayey, and abruptly contact the underlying rock.

87 These results are based on the PRC's second national soil survey, which was aimed at
88 cultivated soils on gentle slopes. Soil resources of mountainous areas were not
89 comprehensively studied. Fully grasping the soil-vegetation relationship and the key
90 controlling factors in the catenary scale are the basic prerequisites for the rational use
91 of scarce soil resources in karst catchments.

92 Soil parent material, special hillslope hydrological processes, and topography, affects
93 catena formation in many ways in karst areas. Three factors are in play: 1) The
94 Southwestern China karst area is low in acid-insoluble and insufficient sources of soil-
95 forming materials in carbonate rocks. When soil-forming materials are extremely
96 scarce, whether it can form a soil catena with obvious soil development sequence? 2)
97 Carbonate bedrock forming slopes are characterized by highly induced porosity
98 resulting in a well-developed underground drainage system. These often outcrop at or
99 near the surface. They facilitate rapidly surface water transport underground, even
100 during rainfall and runoff events (Williams 1983; Feng et al. 2016). Hillslope scale
101 overland flow rarely occurs in karst areas compared to non-karstic areas (primarily
102 silicate rocks). How does this affect the hydrodynamic conditions that drive the
103 downward and lateral migration of soil materials at different topographic positions?
104 Will it affect the differential sorting and redistribution of soil particles across the slope?
105 3) In karst catchment, slopes and depressions, what the characteristics of rapid changes
106 in short distances, and the transition between the two are not obvious. This is clearly
107 different from non-karst area topographic position characteristics, where slope
108 gradually descends and transitions to valley floor, thus forming a long slope. Whether
109 karst slope land is able to form a soil catenary pattern similar to non-karst areas, it
110 remains to be determined by field investigations.

111 Through catenary scale soil and vegetation investigation, the objective of this study
112 was to verify the hypotheses that: (1) dolomite slope can still present a typical soil
113 catena pattern; (2) vegetation communities and soil types are spatially associated in this
114 dolomitic peak-cluster depression catchment.

115 **2. Materials and Methods**

116 **2.1. Study area**

117 This study was conducted in a typical karst catchment located at
118 24°43'58.9"~24°44'48.8"N, 108°18'56.9"~108°19'58.4"E in Mulian, Huanjiang County,
119 Guangxi (Fig. 1). The area is 1.46 km² and an elevation of 272 to 647 m above sea level.
120 It is in a subtropical mountain monsoon climate zone which has an average annual
121 rainfall of 1389 mm. The rainy period is May-October and accounts for 70% of the
122 annual rainfall (Hu et al. 2015). Annual average temperature in this area is between
123 19.6-21.6°C. The lowest temperatures, about 3.4~8.7°C occurs in January -March. The
124 highest, 23.0-26.7°C, in July-September. Slope soil is shallow. Gravel content is high.
125 The soil thickens gradually from slope to depression. Since 1985, the government has
126 carried out a "returning farmland-to-forest" policy. The area is recovering to a natural
127 state. The main trees are *Radermachera sinica*, *Celtis biondii*, *Rhus chinensis*,
128 *Schefflera heptaphylla*. The shrubs are *Vitex negundo* and *Ligustrum lucidum*,
129 *Pyracantha fortuneana*. The precominant herbs are mainly *Miscanthus floridulus*,
130 *Bidens pilosa* and *Pteridium aquilinum*.

131 Mulian catchment is in the western wing of the Mulian anticline. Its aquifer is
132 primarily constituted of middle and late Carboniferous dolomite with a strata
133 orientation of 278°∠10°. It is underlain by an early Carboniferous sandstone aquifer
134 which is relatively impermeable (Fig. 1). The underlying rocks are very pure dolomite

135 rocks. Borehole analysis suggests that karstification degree decreases as depth increases.
136 Study area karstification is characterized by penetrating dissolution pores, micro-tensile
137 dissolution fractures, and local dissolution fractures. Its highly weathered dolomite is
138 mostly lost its original rock structure and even deconstructed into dolomite sand. There
139 is no obvious bubble reaction obtained after dropping dilute hydrochloric acid on it.

140 **2.2. Methods**

141 **2.2.1. Soil, rock, and vegetation characteristics**

142 The four topographical positions along the toposequence in Mulian catchment:
143 upper-, middle- and lower-slopes, and depression were examined for soil, rock, and
144 vegetation characteristics (Fig. 1). At each topographical position, a 400 m² (20 m×20
145 m) vegetation survey plot was established. The 400m² large sample plot was divided
146 into plots: 10 m×10 m for a tree survey; 5 m×5 m for a shrub survey; and 1 m×1 m for
147 an herb layer survey. Species name, height, diameter at breast height and plant number
148 of trees, shrubs and herbs in the investigated plots were recorded.

149 Due to the strong spatial heterogeneity in the karst area, a total of 14 soil pits were
150 used: three for both upper-slope and depression positions, and 4 for both mid-slope and
151 lower-slope positions (Table S1), for soil profiles description and soil samples
152 collection. Soil pits were excavated to the C horizon or the epikarst zone. The main
153 topographic variables, including altitude, slope gradient and gravel content, and soil
154 profile morphological characteristics for each soil pits were recorded and described
155 according to FAO-ISRIC-ISSS (2006) (Wrb 2006). Triplicate bulk soil samples, of
156 about 5 kg, were taken for each soil genetic horizons from all side of the pits. Traditional
157 small metal cylinder with a volume of 100 cm³ were unsuitable for solid cores from
158 rocky soils of this karst catchment. Large PVC tubes with height 15 cm, inner diameter

159 of 10 cm, and a volume 1178 cm³ were fabricated and used as soil cylinders to obtain
160 undisturbed soil samples.

161 A series of boreholes (with a diameter of 15 cm) were made in the upper-, middle-,
162 lower-slopes and depressions in order to study near-surface hydrological processes in
163 the slope-depression system. Borehole core profiles were photographed and described
164 during the drilling process of the sampling of dolomite rocks from the middle-slope and
165 the depression which were collected to analyze chemical composition.

166 ***2.2.2. Determination of soil physical properties***

167 Soil saturated hydraulic conductivity was determination: first by putting the soil
168 cylinder samples into a sink. The sink liquid level of the sink was 2 cm below the upper
169 end of the soil cylinder. Soaking for 12 hours was allowed for the soil to fully absorb
170 water and saturated. Then constant-head method was used to measure soil saturation
171 hydraulic conductivity.

$$172 \quad K_s = \frac{10QL}{A\Delta HT} \quad (1)$$

173 In this formula, K_s (mm/min) is saturated hydraulic conductivity. Q-outflow (ml) is
174 within t time. L (cm) is linear distance of the water flow path. A (cm²) is the water flow
175 cross-sectional area. ΔH (cm) is the total head difference between the beginning and
176 end of the seepage path. T (min) is the outflow time (Yi et al. 2019).

177 Determination of the soil material composition included gravel and fine soil
178 component: Soil cylinder was the total volume of soil material (V_T -cm³). Soil cylinder
179 contents were transferred to an oven baked at 105°C, and dried for 12 hours. And then
180 weigh to obtain total soil cylinder mass. This was the total soil material mass (M_T -g).
181 Gravels, defined as having a diameter > 2 mm were selected and provided the gravel
182 component total mass (m_g -g). What remained was the fine soil component which were

183 components <2 mm. Fine soil mass was expressed as m_f (g). This was ground and
 184 sieved through a 2 mm sieve. Dried cylinders sample gravel was water-soaked for 12
 185 hours fully saturation. Using drainage method determined gravel volume (v_g -cm³)
 186 (Wang et al. 2017). Gravel density (ρ_g -g/cm³) could be calculated as:

$$187 \quad \rho_g = m_g/v_g \quad (2)$$

188 The values determined above were used to calculate fine soil mass ratio (M_F -%),
 189 gravel mass ratio (M_G -%), fine soil volume ratio (V_F -%), and gravel volume ratio
 190 (V_G -%). v_f is fine soil volume (cm³), the formula was as follows:

$$191 \quad v_f = V_T - v_g \quad (3)$$

$$192 \quad M_F = m_f/M_T \times 100\% \quad (4)$$

$$193 \quad M_G = m_g/M_T \times 100\% \quad (5)$$

$$194 \quad V_F = v_f/V_T \times 100\% \quad (6)$$

$$195 \quad V_G = v_g/V_T \times 100\% \quad (7)$$

196 Fine soil texture was determined using the hydrometer method.

197 Soil bulk density (BD), and fine soil bulk density (δ_f) indicated as the bulk density
 198 of the total soil material and of the soil material excluding gravel component,
 199 respectively. They were calculated as follows.

$$200 \quad BD = M_T/V_T \quad (8)$$

$$201 \quad \delta_f = (M_T - m_g)/(V_T - v_g) \quad (9)$$

202 M_T (g) is total soil mass. V_T (cm³) is total soil volume. m_g (g) is gravel mass. v_g (cm³)
 203 is gravel volume.

204 **2.2.3. Calculating of pedon scale average nutrient content and nutrient stocks**

205 There was a significant positive correlation between soil thickness and vegetation
 206 productivity. This correlation became more significant for the soil thickness in the 0-50
 207 cm (Li and Duan 2014). Shallow soil nutrient stocks affect productivity which is not

208 only solely controlled by the soil nutrient content. Karst slope soil was generally
209 shallow. Lower-slope and depression soils were relatively deep. Soil nutrient content
210 may not fully reflect actual soil productivity. This study compared average nutrient
211 content with nutrient stocks within the pedon scale to explore the appropriate index for
212 assessing shallow and high gravel soil productivity in peak-cluster depressions.

213 The soil nutrient content (N_c) parameters include total nitrogen (TN), total
214 phosphorus (TP), total potassium (TK) content, and soil organic matter content
215 parameters which were measured and calculated according using the techniques used
216 by Bao (2000).

217 This study used the calculation method of soil organic carbon stocks presented in the
218 second edition of the "2011 Soil Investigation Laboratory Information Handbook" of
219 the Natural Resources Conservation Service of the United States Department of
220 Agriculture for soil nutrient stocks index (U.S. Department of Agriculture; Fei et al.
221 2015).

222 The PVC tubes, with a volume of 1178 cm^3 , described above to collect soil cylinders
223 were used. These soil cylinders did not all have the same height. The true soil cylinder
224 height was the sum of the fine soil height and gravel height. The gravel height of each
225 soil layer, represented by d_g (cm), fine soil height of each soil layer, represented by
226 d_f (cm). d_g and d_f could be calculated using the actual soil layer thickness, D (cm),
227 for each soil layer. According to the area of PVC tube bottom was equal, so the ratio of
228 gravel volume ($v_g\text{-cm}^3$) to fine soil volume ($v_f\text{-cm}^3$) was consistent with the ratio of
229 gravel height to fine soil height of soil cylinders. The ratio of d_g and d_f is
230 approximately equal the ratio of gravel height to fine soil height for a soil cylinder.
231 Therefore, it was equal to the ratio of gravel volume to fine soil volume. This is the

232 formula:

$$233 \quad v_g/v_f = d_g/d_f \quad (10)$$

$$234 \quad d_g + d_f = D \quad (11)$$

235 According to the gravel height and fine soil height for each soil layer, calculate the
236 gravel volume (V_1 -cm³/m²) and the fine soil volume (V_2 -cm³/m²) of the soil layer per
237 unit area. Gravel density (ρ_g -g/cm³) were used to calculate the mass of gravel per unit
238 area of soil (m_1 -kg/m²). Fine soil bulk density (δ_f -g/cm³) were used to calculate the
239 mass of fine soil per unit area of soil (m_2 -kg/m²). m_t represents the total mass of soil
240 per unit area. This the formula:

$$241 \quad V_1 = d_g \times 10^4 \quad (12)$$

$$242 \quad V_2 = d_f \times 10^4 \quad (13)$$

$$243 \quad m_1 = V_1 \times \rho_g \times 1000 \quad (14)$$

$$244 \quad m_2 = V_2 \times \delta_f \times 1000 \quad (15)$$

$$245 \quad m_t = m_1 + m_2 \quad (16)$$

246 In the calculation of the nutrient stocks per unit area of each soil layer, N_s is the
247 nutrient stocks per unit area for each soil layer measured as kg/m². N_c is the each soil
248 layer nutrient content measured as g/kg. The formula was as follows:

$$249 \quad N_s = m_2 \times N_c \times 1000 \quad (17)$$

250 Pedon scale nutrient stocks is equal to the sum of gravel nutrient stocks and fine soil
251 nutrient stocks for each soil layer, but the gravel nutrient content is extremely low
252 (Table S2), resulting in the low nutrient stocks of gravel, and negligible. Therefore, the
253 nutrient stocks of the pedon scale are equal to the sum of the nutrient stocks of fine soil
254 in each soil layer. Specific values of nutrient content and nutrient stocks for each soil
255 genetic horizons are in Table S3.

256 **2.3 Data analysis**

257 Excel 2019 was used to process data. One-way analysis of variance and Duncan

258 method analyzed soil physical and chemical properties differences. The significance
259 level was set at $\alpha=0.05$. Pearson correlation analysis tested correlation between
260 topographic factors, soil properties, and vegetation factors. Origin 2021 drew related
261 charts.

262 **3. Results**

263 *3.1. Spatial variability of soil formation characteristics along the toposequence*

264 *3.1.1. Soil formation conditions at different topographic positions*

265 Peak-cluster depressions have a unique landform resulting from the long-term
266 karstification process. The hillside abruptly changes into a depression. The height
267 difference from the peak-cluster top to the depression was about 377 m. The slope was
268 about 400 m long. The depression was about 300 m wide. The slope length-to-
269 depression width was about 4:3. Slopes and depressions areas respectively accounted
270 for 64% and 27% of the catchment area. The peak-cluster depression subdivides into
271 four topographic positions. 1) exposed bedrock cliffs with a slope close to 90°. 2) an
272 mostly exposed rock upper-slope with a slope of 32°; a greater exposed rock mid-slope
273 with of 23°; and, less exposed rock lower-slope of 18°.

274 Soil-forming material spatial distributions at different topographic positions show a
275 sorting phenomenon from coarse to fine. Between the cliff and the depression, the large
276 weakly-weathered rock mass changes to a moderately-weathered rock mass, then to
277 strongly-weathered clastic rock ending in dolomitic sand layer (Table 1).

278 The drilling cores's average mass contents for CaO and MgO were about 31% and
279 21%, respectively (Table 1). Average mass content of acid-insoluble account for about
280 0.17% of total rock mass. This suggests a very pure dolomite rocks in this study

281 catchment. As the slope decreases, the soil pH value of the soil gradually decreased
282 (Table 1). Upper-slope and mid-slope soil pH inherited the high alkaline characteristics
283 of the underlying weathered dolomite. Lower-slope soil pH, particularly in depressions,
284 reduced to neutral, or acidic. That soil's properties were less affected by the underlying
285 bedrock.

286 ***3.1.2. Soil profile morphological characteristics in different topographic positions***

287 Soil profile for different topographic positions can be divided into three soil genetic
288 horizons having dissimilar properties. They are a designated A; AC or B; and C. The
289 "A" layer is black surface layer. "AC or B" is a yellow illuvial horizon and "C" is a
290 white dolomite strongly weathered layer (Table 1). There is a deep dolomite weathering
291 layer in the study catchment. The degree of weathering decreases with depth (Table 1).
292 The differences in the degree of dolomite weathering at different topographic positions
293 are that weathering weakest on the upper-slope where the weathered layer was 1.5 m.
294 The thickness of the dolomite strongly weathered layer in other topographic positions
295 from 2.5 m to 10 m. The dolomite weathered layer was dominated by fine sand formed
296 by overall dissolution. There were no large pores, cracks, karst conduits and other
297 structures in the weathered layer. The boundary between soil and dolomite weathering
298 layer was clear to the naked eye. The contact surface between the two showed an
299 extremely irregular wavy shape. No soil particles had migrated vertically through the
300 rock weathering layer. From the upper-slope to the depression, soil profiles property
301 changes were obvious. Soil thickness increased gradually (Table 1). The A-C transition
302 layer become more visible. Gravel content decreased gradually. Soil fine particle
303 proportions gradually increased. Lower-slope and depression soil presented B layer
304 which was an obvious illuvial horizon.

305 Soil profiles development morphology analysis returned that upper-slope soil was
306 entisolic and weakly developed. Differentiation between the various soil layers was not
307 obvious. Upper-slope soil was shallow and black with a high gravel content. Middle
308 slope soil was cambisolic, and soil profile development degrees were low. A light
309 yellow weak illuvial horizon was observed under the black surface layer suggesting a
310 weak eluvial and illuvial process. Lower-slope soils were semi-luvisolic having good
311 drainage. The soil profile was moderately developed and a yellow-brown sedimentary
312 layer was easily detected. Depression soil with a yellow surface was highly developed
313 and alfisolic. It had an apparent illuvial horizon. The lower part of it is affected by
314 lateral seepage and formed calcareous concretions and iron-manganese nodules.

315 ***3.2. Soil physico-chemical characteristics along the toposequence***

316 ***3.2.1. Soil physical properties at different topographic positions***

317 Upper- and middle-slope soil profiles were composed mainly of gravel. Upper slope
318 average gravel mass and volume ratios were 73% and 64% respectively (Fig. 2). In the
319 middle slope these were 78% and 47% respectively. Lower-slope and depression soil
320 profiles were mainly fine soil. Lower-slope gravel mass and volume ratios were 1.30%
321 and 1.09%, respectively. Depression ratios were 0.21% and 0.24%. Gravel mass and
322 gravel volume proportions decreased as slope decreased. Fine soil mass and fine soil
323 proportion volumes showed the opposite trend which are obvious slope colluvium
324 characteristics (Fig. 2).

325 There was a high average clay content of between 32%-52% in lower-slope and
326 depression profiles (Fig. 3). Lower-slope clay content relatively smoothly, with depth
327 (Table 2). Upper and middle slopes have higher sand content which increases with depth.

328 The average profile sand content was between 68% and 81% (Fig. 3). This shows that
329 lower-slope and depression belong to the clay group. Saturated hydraulic conductivity
330 decreased as the soil depth increase (Table 2). Depression saturated hydraulic
331 conductivity was the least with a maximum value only 61 mm/h (Table 1). Middle slope
332 maximum saturated hydraulic reached 5095 mm/h. Dolomite slope land is entisolic
333 with high permeability and well drainage. Depression land soil is alfisolic with low
334 permeability and poorly drained.

335 ***3.2.2. Average nutrient content and nutrient stocks at different topographic positions***

336 If there is a “rule of nutrient content change” along a slope it was not obvious (Fig.
337 4). Soil nutrient stocks gradually increase at different topographic positions. This
338 largely agrees with soil thickness and apparent soil productivity trend changes along
339 the slope. Soil TN (2.07 kg/m²), TP (1.19 kg/m²), TK (9.68 kg/m²), and organic matter
340 (47.68 kg/m²) nutrient stocks were all significantly higher than for the upper- and
341 middle-slopes (Fig. 4). Soils of karst areas are commonly shallow and gravelly, thus
342 pedon scale nutrient stocks may be a more suitable measure than nutrient content to
343 assess soil productivity.

344 ***3.2.3. Nutrient accumulation in A-layer***

345 This study determined that soil nutrient surface accumulation was significant. A layer
346 nutrient, alone, are not an accurate measure of reflect soil fertility and productivity.
347 Upper-slope A layer have the greatest accumulation. It ranges from 63%-85% (Fig. 5).
348 Middle-slope accumulation ranges from 60%-76%. Lower-slope accumulation was
349 between 33%-56% and for depressions it was 22%-26% (Fig. 5). A layer of depression
350 accumulated relatively few nutrients. Along a slope, nutrient accumulate of A layer
351 gradually lessens. From the characteristics of the black soil layer (Table 1) of upper-

352 slope soil profile, it could also be derived that slope pedon scale surface nutrient
353 accumulation was significantly stronger than that of the depression.

354 Upper-slope surface layer fine soil volume was the greatest at 53.64% (Fig. 6).
355 Middle-, lower-, and depression values were 40.96%, 45.10%, and 33.29% respectively.
356 Surface accumulation increased as the amount of fine soil increased except for lower-
357 slopes.

358 ***3.3. Vegetation patterns responses to topographic change***

359 ***3.3.1. Vegetation changes along the toposequence***

360 On the upper-slope, herbs were about 45% of all plants and shrubs about 36% (Table
361 4). On the mid-slope, shrubs were 58% and herbs 26%. On lower-slopes shrubs and
362 herbs were 62% and 23%. In depressions, herbs were 55% and trees were 42%. Number
363 of trees increased as slope decreased. Initially the shrub increased as position decreased
364 and but then decreased. Plant population was greatest on lower-slopes mainly
365 consisting of shrubs and herbs. Middle-slopes had the least number of plants. Shrubs
366 and herbs predominated on upper- and middle-slopes. Depressions were mainly trees
367 and herbs. Vegetation patterns changed from shrubs to trees with the top to bottom of
368 slope.

369 ***3.3.2. Correlation among topographic, soil properties, and vegetation factors***

370 All measured factors were divided into three categories: 1) topographic factors which
371 includes slope position, soil thickness, gravel coverage, and slope; 2) soil properties
372 which includes, among other measures, soil bulk density, fine soil bulk density,
373 saturated hydraulic and conductivity; 3) vegetation factors which includes tree, shrubs
374 and herbs type and number. Topographical factors Sp and Sd significantly negatively

375 correlated to the soil properties of sand, pH, M_G , and m_1 . Topographical factors Sp and
376 Sd significantly positively correlated with Clay, M_F , m_2 , pedon scale nutrient stocks.
377 This suggests that topographic factors have an influence on the variation of soil
378 properties. Sand, pedon scale nutrient stocks, and M_G , significantly correlated with
379 vegetation factors, indicating that soil properties closely relate to vegetation factors.
380 The four parameters in the topographic factors all significantly correlate with the
381 vegetation factors.

382 **4. Discussion**

383 *4.1. Dolomite-slope shallow soil forms a continuous soil catena pattern*

384 In non-karst areas, the weathering of rock is dominated by physical weathering,
385 supplemented by chemical weathering. Weathering usually occurs at, or close to, the
386 surface. Weathering affected deep bedrock physical and chemical characteristics less
387 (Worthington et al. 2016; Beven et al. 2021). Carbonate rock is generally solvable,
388 therefore karst-area chemical rock weathering processes are often stronger than
389 physical weathering processes (Gilfillan et al. 2009, Ford and Williams, 2015). The
390 weakly acidic water continuously dissolves the deep carbonate bedrock. In limestone
391 networks are formed. In dolomite the process is diffuse. This results in greater
392 weathered rock layer depth in karst areas which may vary from 10-1000 m (Hartmann
393 et al. 2017). It also results in more and more robust spatial heterogeneity of the material
394 structure. The drilling core profiles showed that dolomite weathered layer thicknesses
395 could be beyond 50 m. Strongly-weathered and the weakly weathered layers alternated.
396 This result provided field solid evidence to confirm that, in a karst area, the chemical
397 dissolution in carbonate weathering process is dominated.

398 The dolomite showed an overall uniform weathering pattern. The rock outcrops in
399 the hillslopes are relatively low, thus bare rocks are no barriers to the continuous soil
400 distribution. Even where soil was shallow and the dolomite strongly weathered and the
401 weathering layer was thick, the dolomitic weathering was characterized by diffuse and
402 integral dissolution. As a result, karst fissures and conduits were not well developed.

403 Soil was mainly distributed on the surface. Vertical, water-driven migration into
404 underground karst voids was not detected. This suggests that even in strongly-
405 weathered dolomite eluvium pore structures predominate. Water, but not soil particles,
406 channels through small pores. This results in dolomite soil slopes having a soil catena
407 pattern similar to non-karst areas where soil gradually thickens and continuous
408 distributes along a slope.

409 Compared with soil catena developed in non-karst areas, those developed on
410 dolomite slopes have a short average distance between adjacent soil types, while the
411 number of soil types differs less to non-karst areas. Brunner et al. (2004) studied a
412 Ugandan soil catena, which consisted of granites, gneisses and schists of the
413 Precambrian age. The soil catena there was composed of seven primary soil types. The
414 average distance between adjacent soils was 300 m. Deressa et al. (2018) studied a soil
415 catena, which consisted of alluvium, granitic gneiss and basalt. That soil catena had
416 five soil types. The average distance between adjacent soil types was 10 km. Tsai et al.
417 (2010) studied a Taiwan soil catena composed of two-pyroxene andesites and two-
418 pyroxene hornblende andesites. That soil catena had three soil types. The average
419 distance between adjacent soil types was 1833 m. In the instant study, the dolomite soil
420 catena consisted of four soil types. The average distance between adjacent soil types
421 was 33 m.

422 For karst, underground carbonate rock dissolution is significant. Rainfall quickly
423 recharges groundwater. The surface runoff coefficient was far less than non-karst
424 mountain slopes. The stronger karst slope vertical water flow drives soil profiles soil
425 formation processes more quickly than for non-karst slopes. It seems likely that the
426 more rapid vertical water flow present in a dolomite soil profiles replaces the lack of a
427 hydrological driving force resulting from short slopes and a steep topography. A
428 dolomite slope can also present a complete soil catena pattern.

429 The dissolution rate of limestone was 2 to 60 times higher than dolomite (Bai and
430 Wang 2011). Limestone is characterized by highly differentiated dissolution. The
431 fissures and large conduits network structure in the limestone weathered layer were
432 extremely developed. These structures often become preferential channels for material
433 migration underground (Fig. S1). In the limestone zone, the well-developed
434 underground network void structure dominates the underground material migration
435 process. Do these processes weaken soil material continuous distribution patterns on
436 the slope surface? If so, does this weaken any soil catena pattern phenomenon?

437 ***4.2. Spatial correspondences between vegetation, and soil, patterns***

438 Vegetation, and soil, patterns of the dolomitic peak-cluster depressions present a clear
439 spatial correspondence. This is revealed soil catena distribution patterns being
440 compared to vegetation spatial distribution pattern. (Fig. 8). Vegetation patterns can be
441 inferred from soil patterns. The degree of soil development leads to the different
442 structure of vegetation community. This suggests that the different soil types of this soil
443 catena have significantly different vegetation carrying capacities. Herbs were the
444 primary upper-slope entisolic vegetation (Fig. 8). Herb and shrubs were the primary

445 mid-slope inceptisolic vegetation. Shrubs were the primary lower-slope semi-alfisolic
446 vegetation. Trees were the primary depression alfisolic vegetation.

447 Water and soil nutrient limitations were the two primary factors leading to vegetation
448 spatial pattern changes (David A. Robinson et al. 2008). This study coupled the soil and
449 vegetation surveys at a complete catena in the dolomite peak-cluster depressions of
450 catchment. The close relationships between soil, and vegetation, distribution patterns
451 were disclosed. However, research results have yet to accurately determine the key
452 environmental factors controlling the spatial relationships between soil and vegetation
453 described above. This is because soil water-retention capacities and soil nutrient
454 capacities have strong synergism as slope decreases. The upper-slope soil was shallow
455 and more gravelly. Soil profiles water retention capacities were poor. Soil nutrient stocks
456 were low. Depression soil was relatively deep and less gravelly. It had greater water
457 retention capacities. Soil nutrient stocks were higher (Fig. 8). Soil water retention
458 capacities and soil nutrient stocks show the same trend along the toposequence. A
459 simple factor correlation analysis did not distinguish among the relative contributions
460 of soil water-retention and soil nutrient stocks factor to vegetation distribution patterns.
461 Are dolomite peak-cluster depression vegetation distribution patterns caused by soil
462 moisture retention limitations or soil nutrient limitations, or by the interaction of these
463 two limiting factors, or some other reasons? In-depth research through large-scale
464 investigation and sampling and indoor tests are needed to answer these questions.

465 ***4.3. Quantitative index for evaluating shallow soils' productivity in karst regions***

466 Soil productivity is the ability of soil to support plant growth. Where climates are
467 similar, highly abundant vegetation and biomass usually indicates high productivity

468 (Wang et al. 2015). Non-karst area soil, generally, is deeper and less gravelly. Soil
469 amount maybe not an important factor limiting its productivity. Therefore, scholars
470 evaluate soil productivity in the deep soil zone by evaluating soil fertility based on the
471 nutrient content of the surface soil (about 0-20 cm), and reflect soil productivity through
472 soil fertility. For example, wu et al. (2018) assessed the productivity status of the black
473 soil zone by taking 0-20 cm of soil and measuring its nutrient content. For shallow soils
474 like this study, since the total soil amount significantly affects soil productivity, and the
475 shallow soil exhibits significant A-layer nutrient accumulation. Only depend on the A-
476 layer's nutrient content or stock parameters as criteria for assessing soil productivity
477 would significantly overestimate the productivity of the karstic shallow soil.

478 In this study, it was found that the soil nutrient content was high, but the vegetation
479 in the area was low in number and richness, and low in plant species and diversity. This
480 shows that the nutrient content does not accurately reflect the vegetation characteristics.
481 In this regard, we believe that in this karstic shallow soil zone, the nutrient content may
482 not accurately reflect soil fertility. On the contrary, the nutrient stocks that varied along
483 the toposequence showed the same regularity as the vegetation, and the correlation
484 between them was significant. In addition, the indicators affecting nutrient stocks, such
485 as slope position, soil thickness, sand content, clay content, gravel mass ratio, and fine
486 soil mass ratio, showed the same consistent pattern of variation with vegetation, and
487 the correlation analysis also reflected the significant relationship between the above
488 indirect indicators and vegetation. In summary, comparing nutrient content and nutrient
489 stocks, we propose that nutrient stocks is more applicable to assess soil productivity.

490 **5. Conclusions**

491 Dolomite rocks usually present an evenly progressive karstification pattern. This
492 leads to an undeveloped, fissure-conduit network system. Underground soil creep and
493 fill processes were not obvious for these dolomite hillslopes. Soils concentrated at the
494 surface and show a soil catenary pattern similar to that present in non-karst areas. There
495 was a strong spatial association between soil types and dominant vegetation species.
496 Herbs associated with entisols are on the upper-slope. Herbs and shrubs associated with
497 cambisols are on the middle-slope. Shrubs were associated with semi-luvisols are on
498 the lower-slope. Trees were associated with luvisols are on the depression.

499 Considering karst hillslope rocky and shallow characteristics, the amount of fine soil
500 was the critical factor controlling vegetation growth. Nutrient stock parameters, and
501 other, the study of more easily measurable parameters, such as topographic position,
502 soil thickness and, gravel mass ratio may more suitable for assessing soil productivity
503 than soil nutrient content parameters in karst regions.

504 Borehole core characteristics suggest a positive correlation between soil thickness
505 and epikarst thickness. Further research is needed to confirm whether a soil-epikarst-
506 vegetation catenary pattern exists in dolomite karst catchments. This study focused on
507 soil and vegetation relationships along a toposequence in this typical dolomite
508 developed catchment. Dolomite rock and limestone are the two predominant types of
509 carbonate rocks in karst regions. Their lithologic and dissolution characteristics differ.
510 These differences lead to apparent different soil-epikarst structural differences between
511 them. Weather soil-epikarst-vegetation catenary is also obvious in peak-cluster
512 depression catchment developed from limestone but this remains to be elucidated.

513 **Acknowledgments**

514 This study was supported by the National Natural Science Foundation of China
515 (41930866, 42077077, 41671287), the Guangxi Natural Science Foundation of China
516 (2020GXNSFAA297242) and the Central Guided Local Science and Technology
517 Development Fund Project (ZY21195016).

518

519 **References**

- 520 Applegarth M T, Dahms D E (2001) Soil catenas of calcareous tills, Whiskey Basin, Wyoming,
521 USA. *Catena* 42(1):17-38. [http://dx.doi.org/10.1016/S0341-8162\(00\)00116-8](http://dx.doi.org/10.1016/S0341-8162(00)00116-8)
- 522 Bai, X. Y., S. J. Wang (2011) Relationships between soil loss tolerance and karst rocky
523 desertification. *Journal of Natural Resources* 26(8):1315-1322.
524 [http://dx.doi.org/10.1016/S1671-2927\(11\)60313-1](http://dx.doi.org/10.1016/S1671-2927(11)60313-1)
- 525 Bao SD (2000) *Soil agrochemical analysis* (3rd edn.). China Agriculture Press, Beijing
- 526 Beven, K. J., M. J. Kirkby, J. E. Freer, et al (2021) A history of topmodel. *Hydrology and Earth*
527 *System Sciences* 25:527-549. <http://dx.doi.org/10.5194/hess-25-527-2021>
- 528 Boling, A. A., T. P. Tuong, H. Suganda, et al (2008) The effect of toposequence position on soil
529 properties, hydrology, and yield of rainfed lowland rice in Southeast Asia. *Field Crops*
530 *Research* 106:22-33. <http://dx.doi.org/10.1016/j.fcr.2007.10.013>
- 531 Brunner A C, Park S J, Ruecker G R, et al (2004) Catenary soil development influencing erosion
532 susceptibility along a hillslope in Uganda. *Catena* 58(1):1-22.
533 <http://dx.doi.org/10.1016/j.catena.2004.02.001>
- 534 David A. Robinson, Hiruy Abdu, Scott B. Jones, et al (2008) Eco-geophysical imaging of
535 watershed-scale soil patterns links with plant community spatial patterns. *Vadose Zone Journal*
536 7(4):1132-1138. <http://dx.doi.org/10.2136/vzj2008.0101>
- 537 Deressa A, M. Yli-Halla, M. Mohamed, et al (2018) Soil classification of humid western ethiopia:
538 a transect study along a toposequence in Didessa watershed. *Catena* 163: 184–195.
539 <http://dx.doi.org/10.1016/j.catena.2017.12.020>.
- 540 D Ford, Williams P W (2015) *Karst Hydrogeology and Geomorphology*. Wiley.
- 541 Ding, Y. L., Y. P. Nie, H. S. Chen, et al (2021) Water uptake depth is coordinated with leaf water
542 potential, water-use efficiency and drought vulnerability in karst vegetation. *New Phytologist*

543 229:1339-1353. <https://doi.org/10.1111/nph.16971>

544 Fei W, Qin F, Wu D, et al (2015) Comparative study on the calculation method of soil organic matter
545 and organic carbon. *Journal of Agriculture* 5(03):54-58.

546 Feng, T., H. S. Chen, V. O. Polyakov, et al (2016) Soil erosion rates in two karst peak-cluster
547 depression basins of northwest Guangxi, China: Comparison of the RUSLE model with (CS)-
548 C-137 measurements. *Geomorphology* 253:217-224.
549 <http://dx.doi.org/10.1016/j.geomorph.2015.10.013>

550 Gilfillan S, Lollar B S, Holland G, et al (2009) Solubility trapping in formation water as dominant
551 CO₂ sink in natural gas fields. *Nature* 458(7238):614-618.
552 <http://dx.doi.org/10.1038/nature07852>

553 Hartmann, A., T. Gleeson, Y. Wada, et al (2017) Enhanced groundwater recharge rates and altered
554 recharge sensitivity to climate variability through subsurface heterogeneity. *Proceedings of the*
555 *National Academy of Sciences of the United States of America* 114:2842-2847.
556 <http://dx.doi.org/10.1073/pnas.1614941114>

557 Hong-Liang Wu, Wang S C, Sheng-Chang H, et al (2018) Evolutionary characteristics of fertility
558 and productivity of typical black soil in recent 30 years. *Journal of Plant Nutrition and*
559 *Fertilizers* 24(6): 1456–1464. <http://dx.doi.org/10.11674/zwyf.18238>

560 Hu K, Chen H, Nie Y, et al (2015) Seasonal recharge and mean residence times of soil and epikarst
561 water in a small karst catchment of southwest China. *Scientific Reports* 5:10215.
562 <http://dx.doi.org/10.1038/srep10215>

563 Jiang Z (1999) Dynamics features of the epikarst zone and their significance in environments and
564 resources. *Acta Geoscientia Sinica* 20(3):302-308. <http://dx.doi.org/10.3321/j.issn:1006-3021.1999.03.014>

565
566 Jiang, Z., Y. Lian, and X. Qin (2014) Rocky desertification in Southwest China: Impacts, causes,

567 and restoration. Earthence Reviews 132:1-12.
568 <http://dx.doi.org/10.1016/j.earscirev.2014.01.005>

569 Li, A., and X. Duan (2014) Productivity assessment for black soil region in northeastern china using
570 black soil thickness a case study of hebei watershed. Bulletin of Soil and Water Conservation
571 34:154-159. <http://dx.doi.org/10.13961/j.cnki.stbctb.2014.01.044>

572 Liu H, Jiang Z, Dai J, et al (2019) Rock crevices determine woody and herbaceous plant cover in
573 the karst critical zone. Science China Earth Sciences 62: 1756–1763,
574 <https://doi.org/10.1007/s11430-018-9328-3>

575 Lozano-García, B. and Parras-Alcántara, L (2014) Variation in soil organic carbon and nitrogen
576 stocks along a toposequence in a traditional mediterranean olive grove. land degrad. develop
577 25: 297-304. <https://doi.org/10.1002/ldr.2284>

578 Nie Y (1994) Karst development characteristics under the lithologic control of carbonate rocks—a
579 case study in south-central Guizhou. Carsologica sinica (01):31-36. (*in Chinese*)

580 Nie Y P, Chen H S, Wang K L, et al (2011) Seasonal water use patterns of woody species growing
581 on the continuous dolostone outcrops and nearby thin soils in subtropical China. Plant & Soil
582 341(1-2):399-412. <https://doi.org/10.1007/s11104-010-0653-2>

583 Podwojewski P, Poulénard J, Nguyet M L, et al (2011) Climate and vegetation determine soil
584 organic matter status in an alpine inner-tropical soil catena in the Fan Si Pan Mountain, Vietnam.
585 Catena 87(2):226-239. <http://dx.doi.org/10.1016/j.catena.2011.06.002>

586 Schlichting, E (1970) Bodensystematik und Bodensoziologie. Journal of Plant Nutrition and Soil
587 Science = Zeitschrift fuer Pflanzenernaehrung und Bodenkunde 127:1-9.
588 <http://dx.doi.org/10.1002/jpln.19701270102>

589 Sommer, M., and E. Schlichting (1997) Archetypes of catenas in respect to matter - A concept for
590 structuring and grouping catenas. Geoderma 76:1-33. [26](http://dx.doi.org/10.1016/S0016-</p></div><div data-bbox=)

591 7061(96)00095-X

592 Tsai, CC, Chen, et al (2010) Pedogenic development of volcanic ash soils along a climosequence in
593 Northern Taiwan. *Geoderma* 156(1-2):48-59.
594 <http://dx.doi.org/10.1016/j.geoderma.2010.01.007>

595 U.S. Department of Agriculture. Soil Survey Laboratory Information Manual - Soil Survey
596 Investigations Report No. 45 (Version 2.0).

597 Wang J Y, Yan X Y, Gong W (2015) Effect of Long-Term Fertilization on Soil Productivity on the
598 North China Plain. *Pedosphere* 25(3):450-458. <http://dx.doi.org/10.1016/S1002->
599 [0160\(15\)30012-6](http://dx.doi.org/10.1016/S1002-0160(15)30012-6)

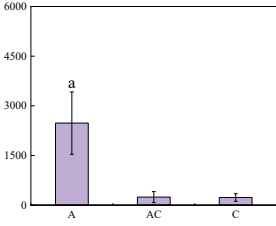
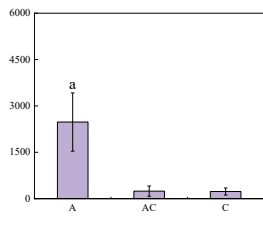
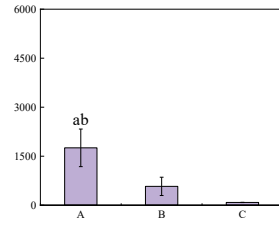
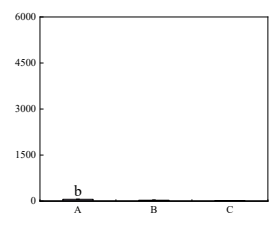
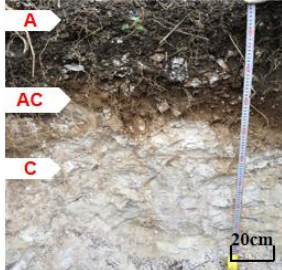
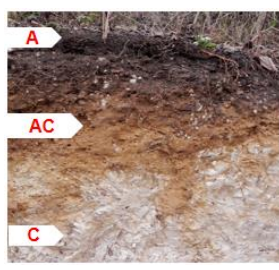
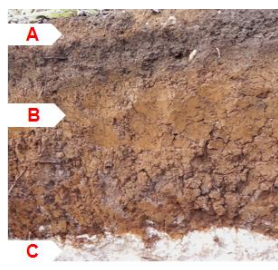
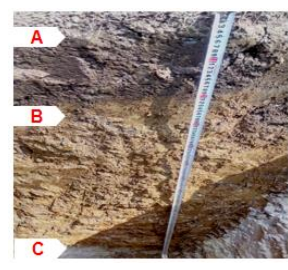
600 Wang X, Cai C, Li H, et al (2017) Influence of rock fragments on bulk density and pore
601 characteristics of purple soil in Three-gorge Reservoir area. *Acta Pedologica Sinica*
602 54(02):379-386. <http://dx.doi.org/10.11766/trxb201601050569>

603 Williams P W (1983) The role of the subcutaneous zone in karst hydrology. *Journal of Hydrology*
604 61(1-3):45-67. [http://dx.doi.org/10.1016/0022-1694\(83\)90234-2](http://dx.doi.org/10.1016/0022-1694(83)90234-2)

605 Worthington S, Davies G J, Alexander E C (2016) Enhancement of bedrock permeability by
606 weathering. *Earth-Science Reviews* 160:188-202.
607 <http://dx.doi.org/10.1016/j.earscirev.2016.07.002>

608 Wrb I (2006) World Reference Base for Soil Resources. A Framework for International
609 Classification, Correlation and Communication. World Soil Resources Reports.

611 **Table 1** Site characteristics, soil hydrological conditions, and soil-rock profile morphology at
 612 different topographic positions

	Upper-Slope	Middle-Slope	Lower-Slope	Depression
Slope gradient (°)	32.06±5.85a	23.00±2.48b	18.46±2.39b	4.40±0.53c
Gravel coverage (%)	45.69±18.20a	50.22±11.92a	16.88±7.56b	7.83±1.02b
Soil thickness (m)	0.56±0.15b	0.70±0.07b	0.76±0.12b	1.18±0.04a
pH	8.11±0.07a	8.12±0.13a	7.35±0.39b	6.89±0.15c
Soil saturated hydraulic conductivity (mm/h)				
Soil profiles photos				
Drill core photos				
Soil types (site drainage)	Entisol (well drained)	Inceptisol (well drained)	Semi-alfisol (moderate drained)	Alfisol (poorly drained)
The chemical composition of parent rock	n.a.	acid insolubles<0.16% CaO-30.91% MgO-21.54%	n.a.	acid insolubles<0.18% CaO-31.15% MgO-21.54%

613 Note: Lowercase (a, b) represent the Anova results in same parameters (p<0.05).

614 n.a.: not analysed.

615 **Table 2** Physical properties of soil genetic horizons for different topographic positions

Topographic position (soil type)	pedon scale	Genetic horizon	Soil thickness (cm)	BD (g/cm ³)	δ_f (g/cm ³)	Sand (%)	Slit (%)	Clay (%)	m ₁ (kg/m ²)	m ₂ (kg/m ²)	m _t (kg/m ²)
Upper-Slope (Entisol)	U1	A	0-25	1.18	0.78	52.66	22.53	24.81	340.38	73.65	414.03
		C	25-59	1.46	1.21	85.13	7.99	6.87	482.67	155.24	637.90
	U2	A	0-17	1.34	1.22	59.74	17.39	22.87	193.19	98.28	291.47
		AC	17-42	1.51	1.24	76.22	7.95	15.83	501.10	70.44	571.54
		C	42-69	1.80	0.62	98.17	1.00	0.83	445.47	52.55	498.03
	U3	A	0-22	1.22	0.45	59.74	16.39	23.87	272.01	45.80	317.81
		AC	22-40	1.83	0.86	96.22	3.05	0.73	335.10	34.38	369.48
		C	>40	n.a.	n.a.	n.a.	n.a.	n.a.	n.a.	n.a.	n.a.
Middle-Slope (Inceptisol)	M1	A	0-22	1.25	0.66	61.62	22.55	15.83	290.82	62.21	353.03
		AC	22-48	1.79	1.34	60.29	20.89	18.82	340.11	125.36	465.47
		C	48-71	1.43	0.34	92.72	7.00	0.28	299.11	34.89	334.00
	M2	A	0-25	1.11	0.58	56.19	19.99	23.82	173.96	103.95	277.91
		AC	25-51	1.36	0.57	61.73	18.40	19.88	267.90	84.65	352.55
		C	51-72	1.56	0.64	91.21	7.93	0.87	255.36	71.07	326.44
		A	0-18	1.29	0.65	60.73	19.40	19.88	151.93	75.59	227.52
	M3	AC	18-53	1.62	0.49	86.25	4.94	8.81	482.63	84.01	566.64
		C	53-75	1.75	0.19	97.22	1.95	0.83	257.06	20.25	277.31
		A	0-40	1.14	0.17	63.72	17.40	18.88	416.34	38.82	455.16
M4	AC	40-60	1.13	0.45	81.12	9.00	9.88	206.00	49.54	255.54	
	C	>60	n.a.	n.a.	n.a.	n.a.	n.a.	n.a.	n.a.	n.a.	n.a.
Lower-Slope (Semi-alfisol)	L1	A	0-20	1.05	1.04	32.31	25.88	41.80	1.17	200.52	201.69
		B	20-45	1.26	1.20	30.31	23.89	45.80	0.33	288.60	288.93
		C	45-80	1.46	1.45	57.64	32.54	9.83	0.01	505.08	505.08
	L2	A	0-25	1.04	1.03	32.23	29.94	37.82	2.98	254.16	257.14
		B	25-61	1.19	1.18	22.28	14.04	63.68	0.00	424.21	424.21
		C	>61	n.a.	n.a.	n.a.	n.a.	n.a.	n.a.	n.a.	n.a.
	L3	A	0-15	1.09	1.08	44.31	20.02	35.67	0.14	162.03	162.16
		B	15-90	1.21	1.20	18.27	13.04	68.69	0.33	901.66	901.99
		C	>90	n.a.	n.a.	n.a.	n.a.	n.a.	n.a.	n.a.	n.a.
	L4	A	0-15	1.05	1.05	44.39	17.99	37.62	0.13	157.14	157.27
		B	15-71	1.17	1.17	35.73	8.4	55.87	0.00	654.11	654.11
		C	>71	n.a.	n.a.	n.a.	n.a.	n.a.	n.a.	n.a.	n.a.
Depression (Alfisol)	D1	A	0-20	1.25	1.25	27.65	32.32	40.03	0.47	249.53	250.00
		B	20-100	1.21	1.21	20.53	30.84	48.63	0.30	965.87	966.17
		C	100-120	1.13	1.33	19.37	30.54	50.09	0.00	265.83	265.83
	D2	A	0-25	1.28	1.28	26.87	32.01	41.12	1.15	317.80	318.95
		B	25-110	1.30	1.30	17.77	36.73	45.5	0.14	1100.54	1100.68
		C	110-120	1.34	1.44	15.34	38.24	46.42	0.00	143.92	143.92
	D3	A	0-28	1.32	1.32	21.03	31.62	47.35	0.55	368.95	369.49
		B	28-97	1.41	1.41	18.41	34.28	47.31	0.28	972.30	972.58
		C	97-113	1.38	1.38	17.38	34.43	48.19	220.73	0.01	0.05

- 616 BD is total soil bulk density. δ_f is fine soil bulk density. m_1 is gravel mass per unit area. m_2 -fine
617 soil mass per unit area. m_t is soil mass per unit area.
618 n.a.: not analysed.

619 **Table 4** Vegetation characteristics for different topographic positions

Topographic positions	Vegetation Types	Number of plant species	Plants number	Percentage(%)
Upper-Slope	trees	3	63	18.10
	shrubs	10	126	36.21
	herbs	3	159	45.69
Middle-Slope	trees	1	41	15.53
	shrubs	7	154	58.33
	herbs	5	69	26.14
Lower-Slope	trees	9	54	13.95
	shrubs	10	241	62.27
	herbs	6	92	23.77
Depression	trees	4	121	42.01
	shrubs	2	7	2.43
	herbs	5	160	55.56

620 The statistics of the above values were on a 400m² sample. Percentage is the ratio different

621 vegetation types to the total plant number.

622 **Figure Captions:**

623 **Fig. 1** Location and geohydrologic background of the study area

624 **Fig. 2** Pedon scale mass ratio and volume ratio of gravel and fine soil for different topographic

625 positions

626 **Fig. 3** Pedon scale grain size distribution of the fine soil fractions for different topographic

627 positions

628 **Fig. 4** Pedon scale average nutrient content and nutrient stocks for different topographic positions

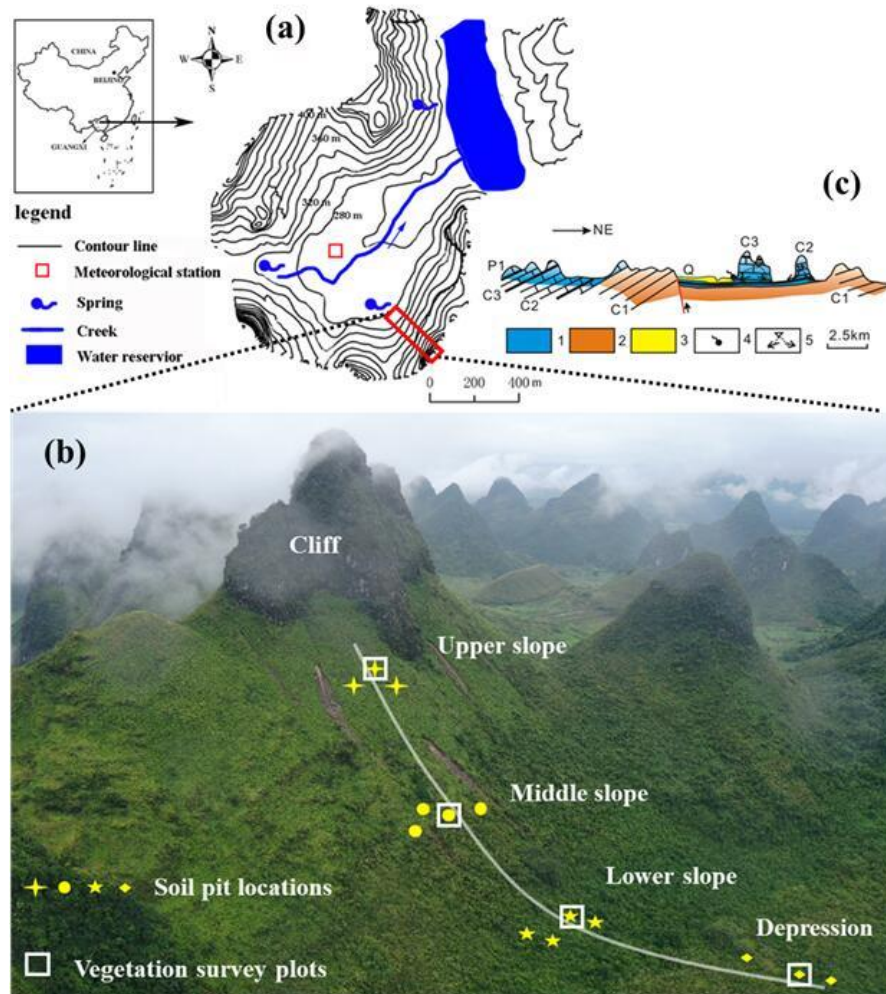
629 **Fig. 5** The ratio of A-horizon's nutrient stock to pedon scale nutrient stocks

630 **Fig. 6** The ratio of A-horizon's fine soil volume to pedon scale fine soil volume

631 **Fig. 7** The correlation between topographic factors, soil properties, and vegetation factors

632 **Fig. 8** A schematic representation of soil catena and its effects on vegetation spatial pattern along

633 the toposequence in the peak-cluster depression catchment developed from dolomite rocks



635

636 (a) Mulian catchment in Huanjiang county, Guangxi, China, topographical map; (b) the peak-cluster

637 depression karst landscape the soil and vegetation locations along the toposequence; and, (c)

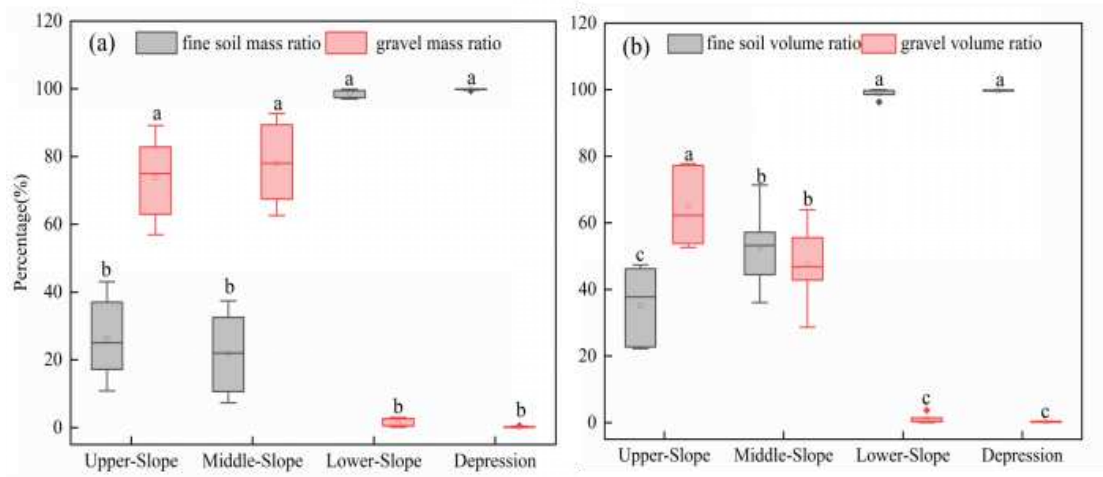
638 geohydrologic background of the study catchment. 1, 2, 3, 4, and 5 indicate the karst aquifer; the

639 sandstone aquifer, a relatively impermeable layer; the porous quaternary aquifer; the spring and

640 ground water flow paths, respectively. P1 is early Permian. Q is Quaternary. C1, C2, and C3

641 indicate the early, middle and late Carboniferous, respectively.

642 **Fig. 1** Location and geohydrologic background of the study area

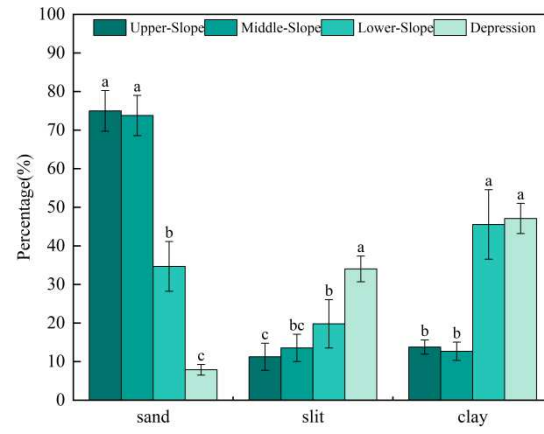


644

645 Note: The lowercase letters indicate significant differences between slope positions ($P < 0.05$).646 **Fig. 2** Pedon scale mass ratio and volume ratio of gravel and fine soil for different topographic

647 positions

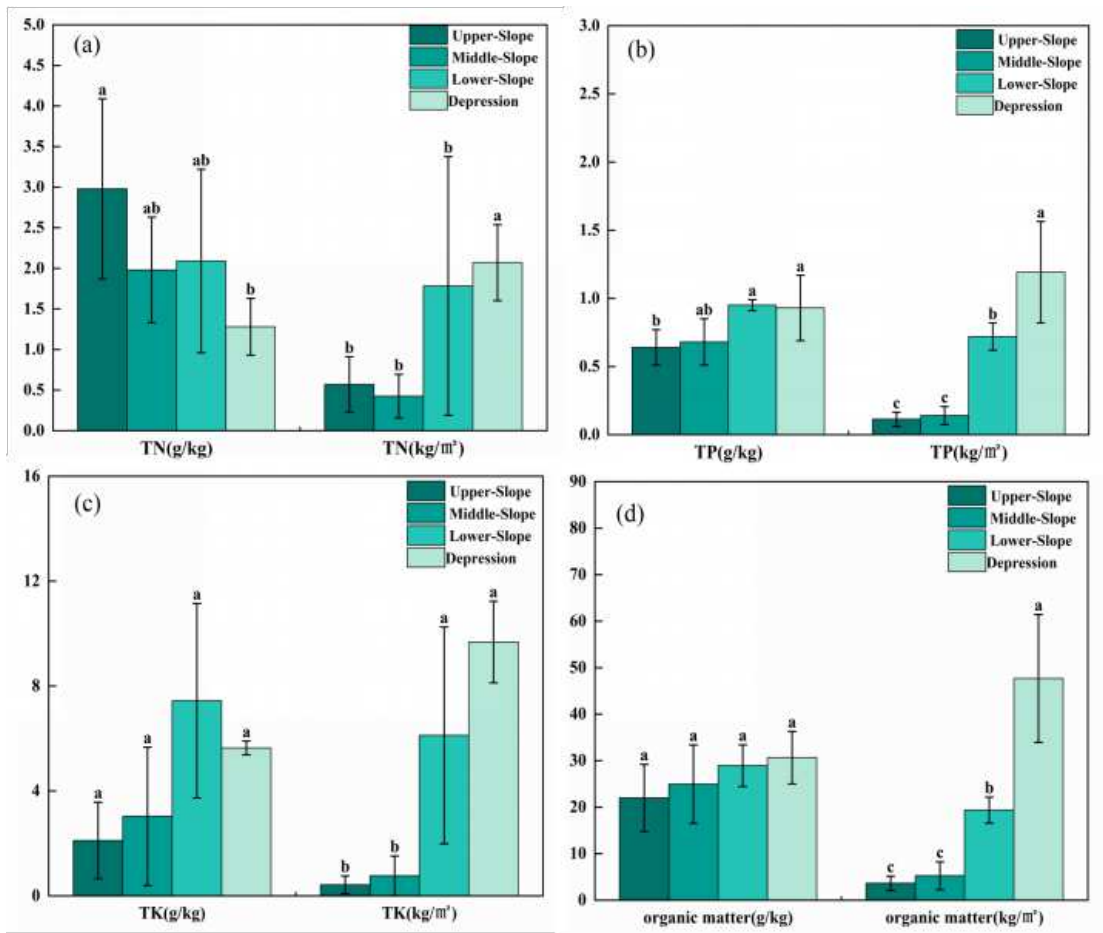
648



650

651 **Fig. 3** Pedon scale grain size distribution of the fine soil fractions for different topographic

652 positions

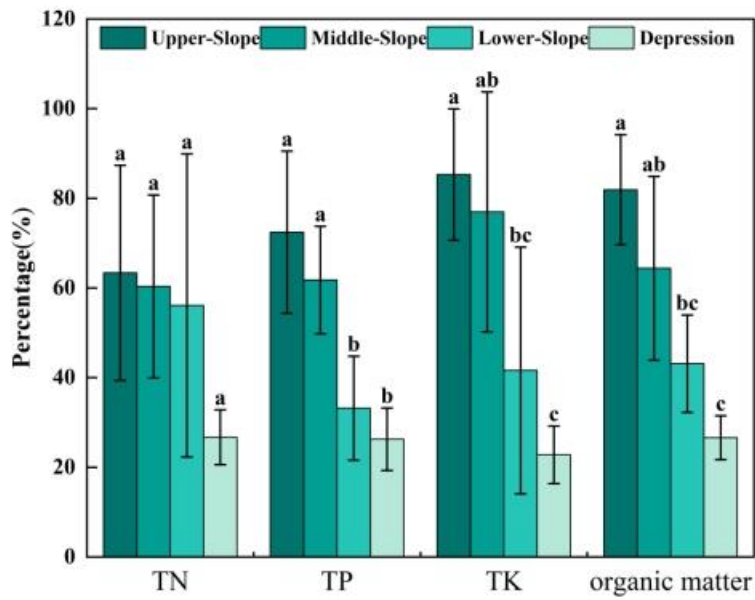


653

654 In Figures a, b, c, and d, the left part represents the nutrient content and the right part represents
 655 the nutrient stocks.

656 **Fig. 4** Pedon scale average nutrient content and nutrient stocks for different topographic positions

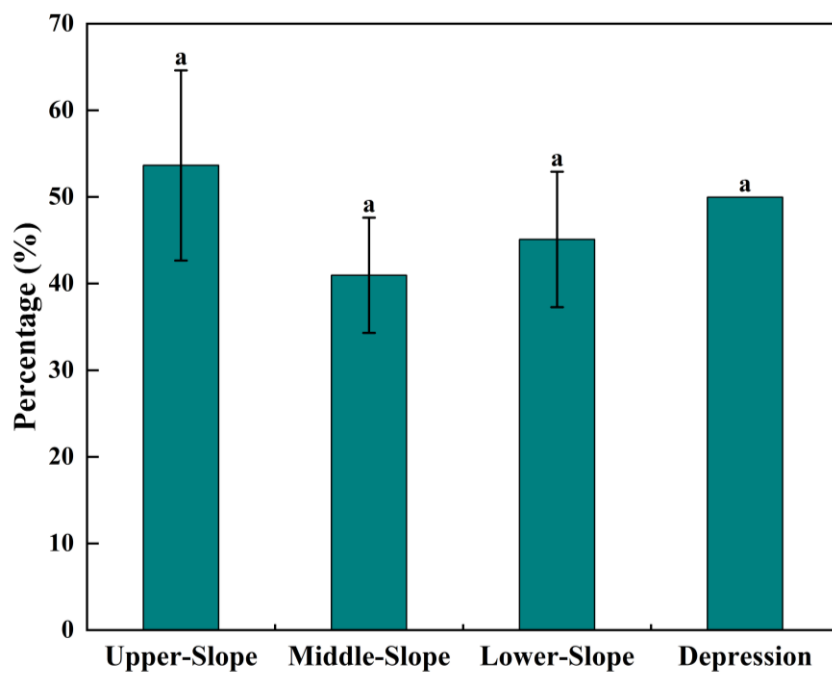
657



658

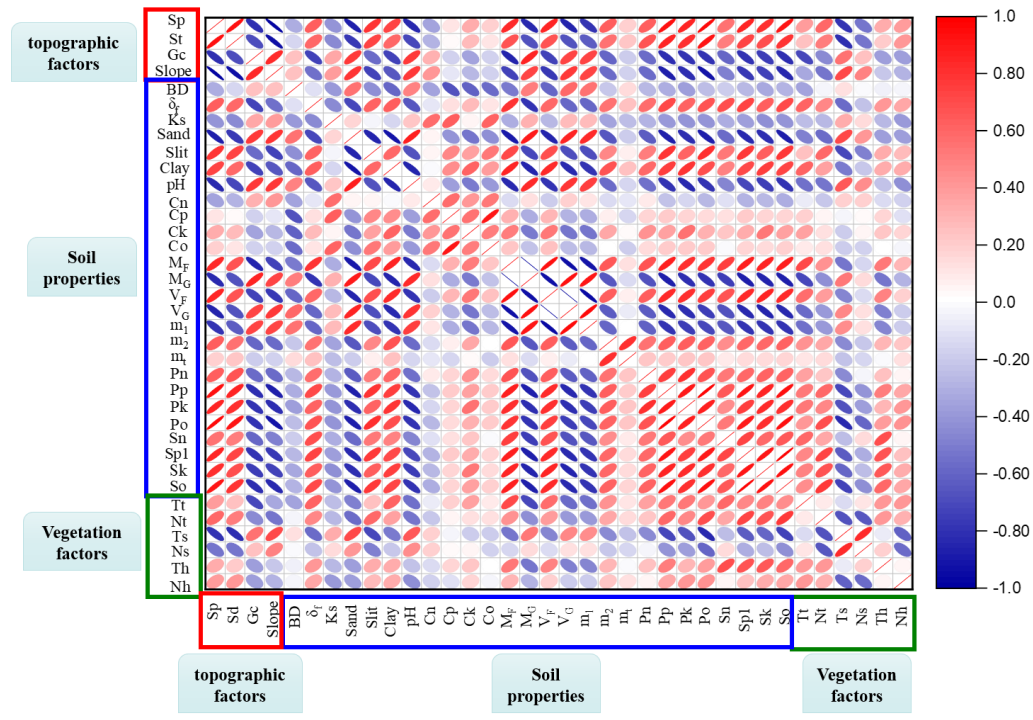
659 **Fig. 5** The ratio of A-horizon's nutrient stock to pedon scale nutrient stock

660



661

662 **Fig. 6** The ratio of A-horizon's fine soil volume to pedon scale fine soil volume



663

664 Note: Sp is slope position. Sd is Soil depth. Gc is gravel coverage. BD is bulk density. δ_f is fine

665 soil BD. Cn is nitrogen content. Cp is phosphorus content. Ck is potassium content. Co is organic

666 matter content. M_F is fine soil content. M_G is gravel content. V_F is fine soil volume ratio. V_G is

667 gravel volume. m₁ is gravel per unit area mass. m₂ is fine soil per unit area mass. m_t is the total

668 mass of soil per unit area, Pn is the pedon total nitrogen stocks, Pp is the pedon total phosphorus

669 stocks, Pk is the pedon total potassium stocks, Po is the pedon organic matter stocks, Sn is the

670 total nitrogen stocks of A layer, Spl is the total phosphorus stocks of A layer, Sk is the total

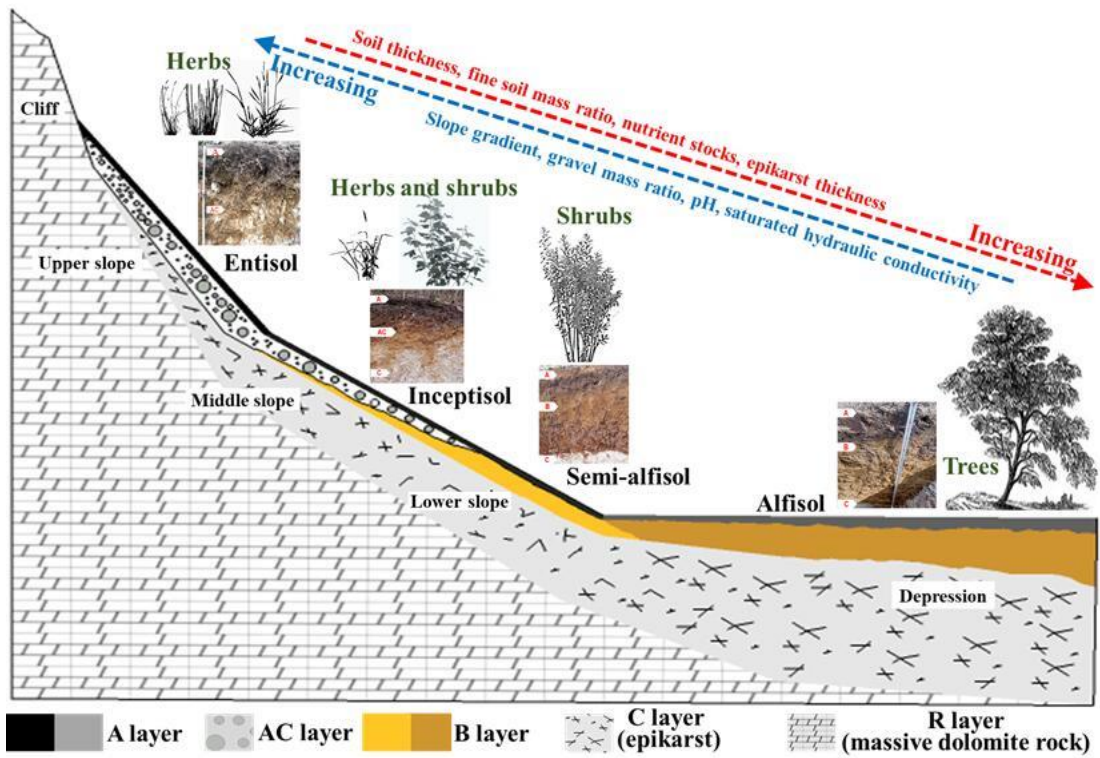
671 potassium stocks of A layer, So is the stocks of organic matter in A layer, Tt is tree types, Nt is the

672 number of trees, Ts is the type of shrub, Ns is the number of shrub, Th is the type of herb, Nh is

673 the amount of herb.

674 **Fig. 7** The correlation between topographic factors, soil properties, and vegetation factor

675



677 **Fig. 8** A schematic representation of soil catena and its effects on vegetation spatial pattern along
678 the toposequence in the peak-cluster depression catchment developed from dolomite rocks

Supplementary Files

This is a list of supplementary files associated with this preprint. Click to download.

- [supplementfile.docx](#)